[^{11}C]4-*N*-Methylamino-4´-hydroxystilbene

[^{11}C]SB-13

The MICAD Research Team

Created: February 27, 2005; Updated: March 3, 2005.

Chemical name:	[^{11}C]4-*N*-Methylamino-4´-hydroxystilbene
Abbreviated name:	[^{11}C]SB-13
Synonym:	
Agent Category:	Compound
Target:	Aggregates of β-amyloid (Aβ) peptides
Target Category:	Acceptor binding
Method of detection:	PET
Source of signal:	^{11}C
Activation:	No
Studies:	• *In vitro* • Non-human primates

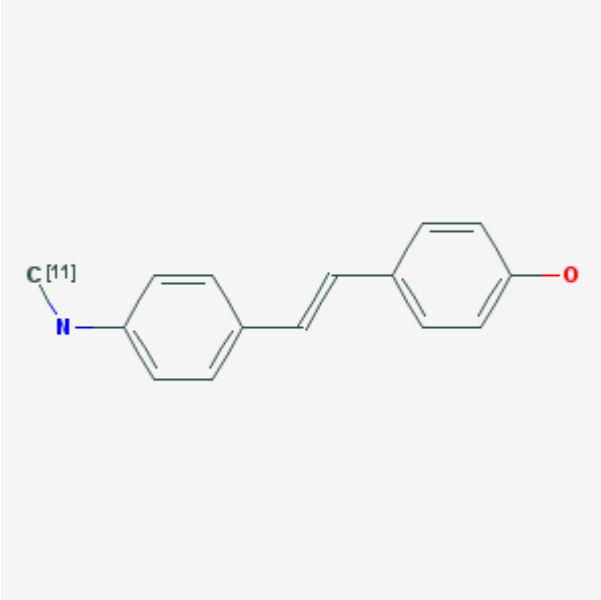

Click on the above structure for additional information in PubChem.

Background

[PubMed]

Alzheimer's disease (AD) is a major neurodegenerative disease associated with an irreversible decline of mental functions and with cognitive impairment (1, 2). It is characterized by the presence, in the brain, of senile plaques of β-amyloid (Aβ) peptides

NLM Citation: The MICAD Research Team. [^{11}C]4-*N*-Methylamino-4´-hydroxystilbene. 2005 Feb 27 [Updated 2005 Mar 3]. In: Molecular Imaging and Contrast Agent Database (MICAD) [Internet]. Bethesda (MD): National Center for Biotechnology Information (US); 2004-2013.

with intracellular neurofibrillary tangles of filaments containing the hyperphosphorylated protein tau (3, 4). Accelerated deposition of Aβ deposits seems to be a key risk factor associated with AD, and although the mechanisms of the disease are still not fully understood, reducing the deposition of amyloid plaques seems to benefit patients.

Several radioligands for positron emission tomography (PET) have been developed (5-7) and tested in humans as *in vivo* diagnostic tools for imaging and measuring the formation and Aβ deposits (7). The first successful agent used in human studies was [^{18}F]FDDNP (8), a malonitrile derivative found to bind to both neurofibrillary tangles and β-amyloid plaques. The second successful attempt was made with [^{11}C]PIB (9), also known as Pittsburgh Compound B or [^{11}C]6-OH-BTA-1. [^{11}C]PIB showed marked retention in areas of association cortex known to contain substantial amounts of Aβ deposits. The third PET radioligand tested in humans was [^{11}C]4-*N*-methylamino-4′-hydroxystilbene, a stilbene derivative commonly named [^{11}C]SB-13.

SB-13 can be labeled with either I-123 or C-11 for *in vivo* imaging using photon emission computerized tomography or PET. Research studies reported in the literature showed that [^{11}C]SB-13 has selective high-affinity binding to amyloid plaques and demonstrated *in vivo* properties similar to those of [^{11}C]PIB when used in AD patients.

Synthesis

[PubMed]

[^{11}C]SB-13 can be synthesized from 4-amino-4′-hydroxystilbene and [^{11}C]methyl triflate, as described by Ono et al. (10). The synthetic procedure uses the ”LOOP” method by which trapping and reaction of the [^{11}C]-methylating agent and precursor are performed inside a high-performance liquid chromatography loop (11). In their experiments, the authors were able to obtain the final product, [^{11}C]SB-13, with a radiochemical yield ranging from 13 to 15% (uncorrected, from [^{11}C]CO_2) and a total synthesis time of 23 min. The radiochemical purity obtained was >98%, and the specific activity at the end of the procedure ranged from 40 to 60 GBq/mmol (1,081 to 1,621 mCi/μmol).

A measure of the partition coefficient (P) for [^{11}C]SB-13 (between 1-octanol and phosphate buffer at pH 7.4), following the described method (12), led to a moderate log(P) of 2.36 ± 0.04, suitable for brain imaging.

In Vitro Studies: Testing in Cells and Tissues

[PubMed]

In vitro binding assays using preformed Aβ aggregates showed that [^{11}C]SB-13 had very good binding affinities for amyloid plaques while competing with the radioiodinated benzothiazole [^{125}I]2-(4′-dimethylaminophenyl)-6-iodobenzothiazole ([^{125}I]TZDM). Its inhibition coefficient (K_i) was found to be 6.0 ± 1.5 nM (at 25 °C) (10). In another

experiment using brain sections of double-mutation mice (TgCRDN8) containing thioflavin S-positive Aβ plaques (10), [11C]SB-13 showed excellent binding properties in the mutant mouse section, whereas binding to the plaques in the control section was minimal (10).

Animal Studies

Rodents

[PubMed]

Ono et al. (10) showed that, in normal rat brains, [11C]SB-13 had moderate lipophilicity (log(P) = 2.36) and very good brain penetration as well as washout after intravenous injection of the radiotracer.

Initial brain uptake was relatively high in the cortex region (~1.5% of injected dose (ID)/g tissue at 2 min post injection), whereas retention was low in the cerebellum regional brain (~0.3% ID/g tissue at 60 min post injection).

Other Non-Primate Mammals

[PubMed]

No publication is currently available.

Non-Human Primates

[PubMed]

No publication is currently available.

Human Studies

[PubMed]

The first human data on [11C]SB-13 were obtained by Verhoeff et al. (13), who studied five female AD patients (53-74 years of age) and six healthy females for comparison (54-77 years of age). A 2-h scan was performed after injection of 370 MBq (10 mCi) of either [11C]SB-13 or the previously known tracer [11C]PIB for comparison. Kinetic analyses were made based on the time–activity curves to obtain Aβ binding-potential estimates, using as input function the unmetabolized tracer concentration in venous plasma (or the density of radioactivity in the cerebellum) from a two-compartment model. As shown previously for [11C]PIB, the standardized uptake value (SUV) for [11C]SB-13 in the cerebellum (~1.75) appeared similar for both control and AD patients, supporting the fact that the cerebellum could be used as a reference region for nonspecific binding.

For a period of 40-120 min after injection of [^{11}C]SB-13 in AD patients, the highest SUVs were obtained in the right striatum (~2.32) and left frontal (~2.35), followed by the right frontal (~2.25) and right thalamus (~2.23). Similar to what was observed for [^{11}C]PIB (9, 14), [^{11}C]SB-13 displayed good blood–brain barrier permeability and substantial retention in affected cortices (e.g., frontal cortex) of AD patients in comparison with control subjects. The relative cortical uptake was higher for [^{11}C]SB-13 than for [^{11}C]PIB.

Relatively high specific/nondisplaceable tissue ratios at equilibrium (Rv), with the cerebellum used as reference, were obtained in the association cortices for both tracers. Those results were found consistent with the fact that, in AD patients, the association cortices contain increasingly dense Aβ plaque accumulations. Obtained Rv values for the right striatum were as follows: ~0.32 for [^{11}C]SB-13 and ~0.72 for [^{11}C]PIB. For the right thalamus, those values were ~0.32 for [^{11}C]SB-13 and ~0.51 for [^{11}C]PIB.

Verhoeff et al. (13) pointed out several limitations in their study, with respect to the modeling of Aβ binding. The first was the polymerization, diffusion, and degradation of the Aβ plaques. Indeed, although [^{11}C]SB-13 likely binds to fibrillar Aβ, there is still controversy about which Aβ species are most important for AD pathogenesis. In addition, the ability of the tracer to penetrate very dense Aβ plaque aggregates likely depends on the shape and size of the plaque.

References

1. Heininger K. A unifying hypothesis of Alzheimer's disease. IV. Causation and sequence of events. Rev Neurosci, 11 Spec No: p. 213-328. 2000.
2. Forstl H, Kurz A. Clinical features of Alzheimer's disease. Eur Arch Psychiatry Clin Neurosci. 1999;249(6):288–290. PubMed PMID: 10653284.
3. Hardy J. The relationship between amyloid and tau. J Mol Neurosci. 2003;20(2):203–206. PubMed PMID: 12794314.
4. Brandt R, Leschik J. Functional interactions of tau and their relevance for Alzheimer's disease. Curr Alzheimer Res. 2004;1(4):255–269. PubMed PMID: 15975055.
5. Nordberg A. PET imaging of amyloid in Alzheimer's disease. Lancet Neurol. 2004;3(9):519–527. PubMed PMID: 15324720.
6. Bacskai BJ, Hickey GA, Skoch J, Kajdasz ST, Wang Y, Huang GF, Mathis CA, Klunk WE, Hyman BT. Four-dimensional multiphoton imaging of brain entry, amyloid binding, and clearance of an amyloid-beta ligand in transgenic mice. Proc Natl Acad Sci U S A. 2003;100(21):12462–12467. PubMed PMID: 14517353.
7. Wu C, Pike VW, Wang Y. Amyloid imaging: from benchtop to bedside. Curr Top Dev Biol. 2005;70:171–213. PubMed PMID: 16338342.
8. Shoghi-Jadid K, Small GW, Agdeppa ED, Kepe V, Ercoli LM, Siddarth P, Read S, Satyamurthy N, Petric A, Huang SC, Barrio JR. Localization of neurofibrillary tangles and beta-amyloid plaques in the brains of living patients with Alzheimer disease. Am J Geriatr Psychiatry. 2002;10(1):24–35. PubMed PMID: 11790632.
9. Klunk WE, Engler H, Nordberg A, Wang Y, Blomqvist G, Holt DP, Bergstrom M, Savitcheva I, Huang GF, Estrada S, Ausen B, Debnath ML, Barletta J, Price JC, Sandell

J, Lopresti BJ, Wall A, Koivisto P, Antoni G, Mathis CA, Langstrom B. Imaging brain amyloid in Alzheimer's disease with Pittsburgh Compound-B. Ann Neurol. 2004;55(3):306–319. PubMed PMID: 14991808.

10. Ono M, Wilson A, Nobrega J, Westaway D, Verhoeff P, Zhuang ZP, Kung MP, Kung HF. 11C-labeled stilbene derivatives as Abeta-aggregate-specific PET imaging agents for Alzheimer's disease. Nucl Med Biol. 2003;30(6):565–571. PubMed PMID: 12900282.
11. Wilson AA, Garcia A, Jin L, Houle S. Radiotracer synthesis from [(11)C]-iodomethane: a remarkably simple captive solvent method. Nucl Med Biol. 2000;27(6):529–532. PubMed PMID: 11056365.
12. Wilson AA, Jin L, Garcia A, DaSilva JN, Houle S. An admonition when measuring the lipophilicity of radiotracers using counting techniques. Appl Radiat Isot. 2001;54(2):203–208. PubMed PMID: 11200881.
13. Verhoeff NP, Wilson AA, Takeshita S, Trop L, Hussey D, Singh K, Kung HF, Kung MP, Houle S. In-vivo imaging of Alzheimer disease beta-amyloid with [11C]SB-13 PET. Am J Geriatr Psychiatry. 2004;12(6):584–595. PubMed PMID: 15545326.
14. Klunk WE, Engler H, Nordberg A, Bacskai BJ, Wang Y, Price JC, Bergstrom M, Hyman BT, Langstrom B, Mathis CA. Imaging the pathology of Alzheimer's disease: amyloid-imaging with positron emission tomography. Neuroimaging Clin N Am. 2003;13(4):781–789. PubMed PMID: 15024961.